Rotating magnetic field experiments in a pure superconducting Pb sphere

Saül Vélez, Antoni García-Santiago,* Joan Manel Hernandez, and Javier Tejada
Grup de Magnetisme, Departament de Física Fonamental, Facultat de Física, Universitat de Barcelona, c. Martí i Franquès 1, planta 4, edifici nou, 08028 Barcelona, Spain and Institut de Nanociència i Nanotecnologia IN2UB, Universitat de Barcelona, c. Martí i Franquès 1, 08028 Barcelona, Spain
(Received 6 August 2009; published 5 October 2009)

The magnetic properties of a sphere of pure type-I superconducting lead (Pb) under rotating magnetic fields have been investigated in different experimental conditions by measuring the voltage generated in a set of detection coils by the response of the sample to the time variation in the magnetic field. The influence of the frequency of rotation of the magnet, the time it takes to record each data point and the temperature of the sample during the measuring process is explored. A strong reduction in the thermodynamic critical field and the onset of hysteretical effects in the magnetic field dependence of the amplitude of the magnetic susceptibility are observed for large frequencies and large values of the recording time. Heating of the sample during the motion of normal zones in the intermediate state and the dominance of a resistive term in the contribution of the Lenz's law to the magnetic susceptibility in the normal state under time varying magnetic fields are suggested as possible explanations for these effects.

DOI: 10.1103/PhysRevB.80.144502 PACS number(s): 07.55.Db, 74.25.Bt, 74.25.Ha, 74.25.Op

Irreversibility phenomena in the intermediate state (IS) of type-I superconductors have received much attention in recent times, following both theoretical and experimental approaches.[1–5] These works have helped to establish the existence of an equilibrium topology in the IS consisting in a tubular structure instead of the laminar pattern that had been believed in the beginning to be the characteristic feature of that state.[6] Dynamical studies, including magneto-optical imaging, in lead (Pb) samples of different shapes have shown that lamellae and stripes are in fact nonequilibrium structures mostly associated to flux exit when the magnetic field is applied parallel to the axis of revolution of disks and cylinders.[7–12] Among the time-dependent phenomena related to the IS, early works centered on different magnetic properties of rotating superconductors, as the generation of magnetic fields and eddy currents.[13–16] However, there is lack to our knowledge of a comprehensive study of the opposite,[17] that is, the dynamics of the normal zones in the IS of type-I superconductors under strong magnetic fields rotating at different angular velocities.

We present here results for a sphere with a radius of 1.5 mm produced by slowly eroding with a whetstone a commercial rod of extremely pure lead (99.999 at. %).[18] In spite of the high purity, the surface of the sample was full of impurities because of the high reactivity of this element during the preparation. Therefore, before starting the experiments a chemical treatment based on acid (HCl is the most efficient) was made in order to clean the surface. The material was covered afterward with a commercial nonmagnetic lubricant to avoid further oxidation in contact with the environment. The sample was then characterized in a commercial superconducting quantum interference device magnetometer[19] by measuring isothermal first magnetization curves at temperatures from 2 to 7 K. Fitting the thermal dependence of the thermodynamic critical field obtained from these curves to the theoretical expression $H_c(T) \approx H_{c0}[1-(T/T_c)^2]$,[20] allowed to determine a value of 802 ± 2 Oe for H_{c0} and a value of 7.23 ± 0.02 K for the superconducting transition temperature, T_c.

The experimental setup shown in the left panel of Fig. 1 is basically a cryostat made on purpose to work in combination with a strong rotating magnetic field[21] and it has already proven useful for studying excited spin states in molecular magnets.[22] The system is fed by a continuous flow of ^{4}He which is controlled by a needle valve that, together with a heater placed close to the sample position (not shown in the figure), allows to achieve very stable temperatures down to 2 K. The cryostat seats inside the bore of a hollow cylindrical $Nd_2Fe_{14}B$ permanent magnet that is set to rotate to create a magnetic field in the xy plane whose modulus varies along the z direction following a negative gradient when moving away from the center of the magnet. The intensity of the magnetic field, H, experienced by the sample can thus be changed from close to zero to near 1 T by moving up and down in a stepwise mode the mechanical support that holds the sample (see the right panel in Fig. 1). A magnetic field profile that gives precisely the value of H as a function of the position along z can therefore be obtained using a micro-Hall sensor in place of the sample.

The sample holder consists in a long tube made of an insulating material,[23] at the end of which a plastic cylinder is appended with its axis parallel to the axis of the tube. A hollow cylindrical space is carved at the lowest part of the lateral surface of the plastic cylinder, being the axes of both perpendicular. The sample was placed in the center of two concentric handmade detection coils with different diameters (4.5 and 7.5 mm) that were lodged inside this cavity. Every coil is composed of three layers, each of which has 30 loops of a 0.1-mm-thick copper wire and was prepared with extremely high accuracy so that every turn in each layer lay close to the neighboring turns without overlapping or leaving blank spaces in between. The aim of this procedure was to have a set of detection coils as sensitive as possible to be used in the experiments described below. Once the sample

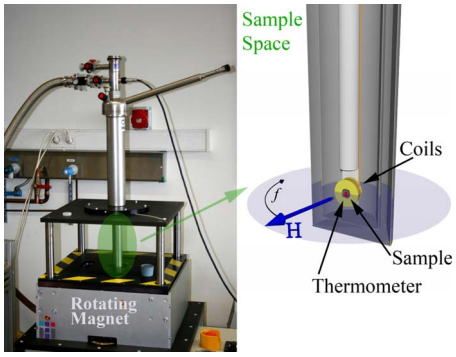

FIG. 1. (Color online) (Left panel) Experimental setup showing the cryostat, the location of the rotating magnet and the whole housing. (Right panel) Detail of the sample holder, showing the configuration of the magnetic field, the location of the sample, the position of the detection coils, and the thermometer that monitors the temperature at the sample surface.

had been placed inside the coils, the system was cooled down to a set temperature, T_{set}, and the magnet was then put to rotate at a frequency f that, after an initial transient regime of a few seconds, achieved a constant stable value. The temperature at the sample surface, T_{sur}, was monitored during the experiments using a commercial low-temperature-sensitive RuO_2 thermometer[24] in close contact.

The signals of both detection coils were registered by a two-channel digital oscilloscope.[25] The voltage of the outer coil, V_{oc}, was displayed in the first channel and was used as a reference for the magnetic field H because it was proportional to the time variation in the magnetic flux through the coil, $d\phi/dt$, and it was nearly insensitive to changes in the sample magnetization, M. The voltage of the inner coil, V_{ic}, reflected instead both the contribution of H and M. The second channel displayed the result of amplifying and subtracting electronically both voltages to eliminate the contribution of dH/dt and obtain a signal proportional to dM/dt. Due to the rotation of the magnetic field, the signals in the channels of the oscilloscope were sinusoidal in time. As a consequence of Faraday's law of induction, it is then expected that all amplitudes will depend linearly on f. Hence, the magnetic susceptibility of the sample, χ, should be simply proportional to the peak-to-peak amplitude of the second channel divided by H and f.

A specific computer program was designed to control the heater, monitor the thermometer, and capture the oscilloscope readings. The program records the magnetic field dependence of both the amplitude and the phase of each channel at constant values of T_{set} and f. The phase difference between both channels when the sample was in the pure superconducting Meissner state (MS) was $\sim\pi$ while its value in the normal state (NS) was $\sim-\pi/2$ due to a residual signal related to the lack of a precise compensation between the two coils.[26] The program also controls the motion of the sample holder along the axis of the cryostat to guarantee that the displacement and the time needed for this change are always the same between any two subsequent experimental points.

Two kinds of measurements were performed at $T_{set}=3$ and 5 K, for frequencies from 350 to 1500 rpm (4.3 to 25.0 Hz). In a first run, once the system had attained one of these T_{set} values, the heater and the needle valve of the cryostat were locked to avoid the equipment recovering the initial state in case a deviation of T_{sur} from T_{set} would be detected by the thermometer and then a waiting time, t_w, was imposed before each experimental point was measured after the sample holder had stopped at a certain position within the magnetic field gradient. In a second run, labeled $t_w \to \infty$, the needle valve and the heater were allowed to act so as to keep T_{sur} always constant and equal to T_{set} during the experiment, and each point was measured just after the thermometer had become stable at $T_{sur}=T_{set}$ in case a temperature deviation had occurred. The average time needed to record every data point in both sets of measurements, including the displacement to the position at which the next data point had to be acquired, was 1 s. In a different kind of experiment, the data were taken continuously at an average rate of 7–8 points per second, just as the magnetic field changed up and down between zero and its maximum value. In this case, only the amplitude of the signal was recorded using a sourcemeter[27] instead of the digital oscilloscope, at several values of T_{set} between 2.3 and 5.5 K, for the largest value of the rotation frequency, $f=1500$ rpm, for which the signal-to-noise ratio was maximum.

Figure 2 shows the magnetic field dependence of the amplitude of the magnetic susceptibility, $|\chi|$, measured at $T_{set}=5$ K for $f=350$, 700, 1100, and 1500 rpm (from left to right and from top to bottom) and $t_w=0$ (solid squares), $t_w=3$ s (open circles), $t_w=10$ s (solid upward triangles), and $t_w \to \infty$ (open downward triangles). Similar results were obtained at $T_{set}=3$ K. Two curves were measured at each pair of f and t_w values, a first one while the magnetic field increased from zero to its maximum value [ascending branch, $|\chi|_{asc}(H)$] and a second one when the magnetic field followed the opposite way [descending branch, $|\chi|_{des}(H)$]. All the signals obtained for each frequency present an initial nearly constant plateau that corresponds to the MS, $\chi \simeq -3/2$, after having taken into account the theoretical value of the demagnetizing factor of a sphere, $N=1/3$.[28] Two characteristic magnetic fields can be distinguished at the points at which $|\chi|_{asc}(H)$ changes slope, from the MS to the IS, what is usually labeled H_c', and from the IS to the NS, that is, the thermodynamic critical field, H_c. A close inspection of all curves shows that H_c' is nearly constant at all f and t_w values, and is very similar to the estimate that can be made from the figures given above for H_{c0}, T_c, and N.

On the contrary, H_c presents a relevant decreasing dependence on both magnitudes, as illustrated in Fig. 3, where the values of H_c extracted from Fig. 2 are plotted as a function of the finite values of t_w, for the different rotating frequencies. The results show that H_c is nearly constant at 350 rpm and is actually very close to the value obtained by measuring the isothermal first magnetization curve at $T_{set}=5$ K while it shows a distinctly decreasing dependence on t_w at any other frequency, indicating a reduction in the magnetic field range at which the IS occurs. The influence of f and t_w can be further explored in Fig. 2 when $|\chi|_{asc}(H)$ and $|\chi|_{des}(H)$ are considered together. In particular, all curves are largely superimposed at the two lowest frequencies while large differ-

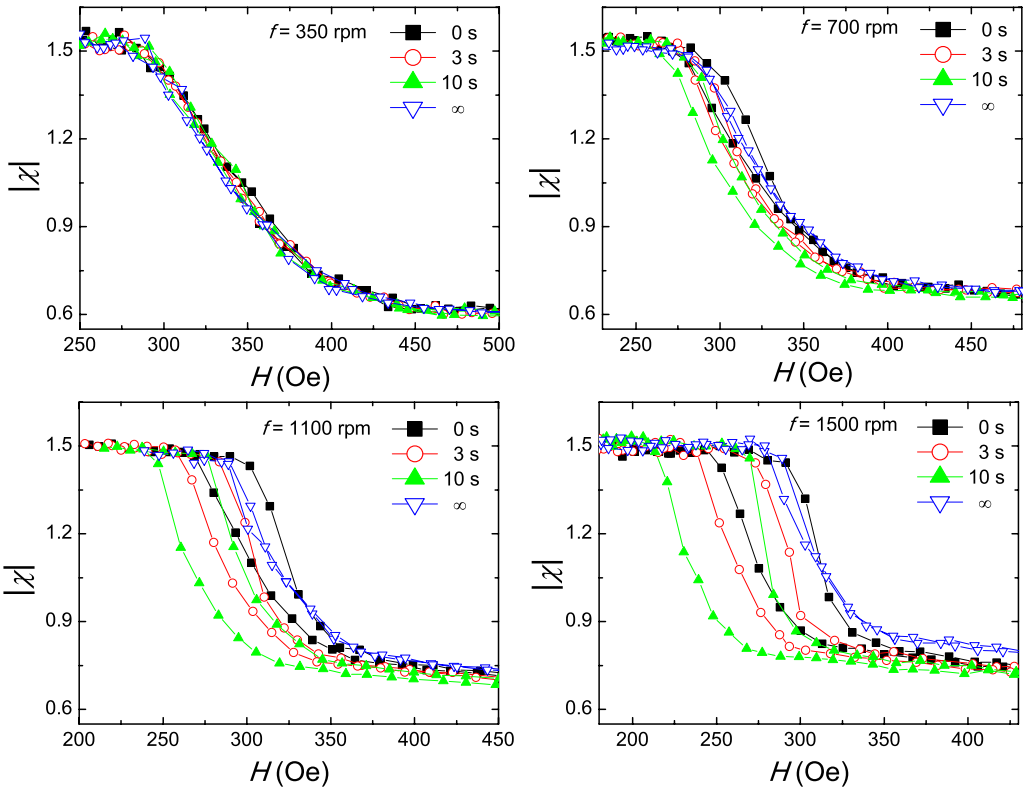

FIG. 2. (Color online) Amplitude of the magnetic susceptibility χ measured as a function of the magnetic field H at a set temperature $T_{set}=5$ K when the permanent magnet rotates at different frequencies (from left to right and from top to bottom): $f=350$, 700, 1100, and 1500 rpm. The curves shown in each panel correspond to different values of the time the system waits before each experimental point is measured: $t_w=0$ (solid squares), $t_w=3$ s (open circles), $t_w=10$ s (solid upward triangles), and $t_w\to\infty$ (open downward triangles). Lines are guides to the eye.

ences are observed at the two highest ones, not only among the curves at different waiting times but also between the ascending and descending branches at each t_w, when hysteresis settles in, with a width that increases with the waiting time.

All these results can be understood if heating of the sample by eddy currents associated to the magnetic field-driven motion of the normal zones in the IS is considered. For magnetic field intensities below H_c', the sample is in the MS and there are not normal zones that can move and dissipate. In this situation, the sample temperature stays close to T_{set} at all f and t_w values and all curves do superimpose. As the magnetic field exceeds H_c', normal zones appear in the sample and tend to move at ever mounting velocities as the magnet rotates faster. As a consequence, the actual temperature of the sample deviates increasingly from $T_{set}=5$ K and H_c is reduced with respect to its theoretical value at this temperature. According to this, the rising influence of the finite waiting time for increasing values of f could be explained by noting that the amount of heat released before each data point is measured increases with t_w, preventing the sample temperature from regaining T_{set} along $|\chi|_{asc}(H)$ and therefore enhancing the reducing effect upon H_c.

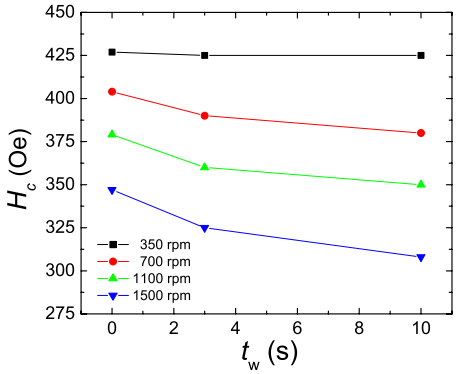

FIG. 3. (Color online) Finite waiting time dependence of the thermodynamic critical field, H_c, at $T_{set}=5$ K, for the different values of the rotating frequency (from top to bottom): $f=350$, 700, 1100, and 1500 rpm. Lines are guides to the eye.

This would also suggest that, for the largest values of f and t_w, the system would follow an excursion through a series of states lying on the descending branches of the different hysteresis cycles corresponding to subsequently increasing values of the sample temperature due to the large amount of heat released. The results obtained at $t_w\to\infty$ help to corroborate this interpretation: as each experimental point is taken only once T_{sur} is set back to T_{set}, the sample describes a succession of equilibrium states that superimpose for increasing and decreasing magnetic fields, and should thus match those corresponding states in the magnetization curve at $T_{set}=5$ K. It is however interesting to observe that the value determined experimentally for H_c from $|\chi|_{asc}(H)$ turns

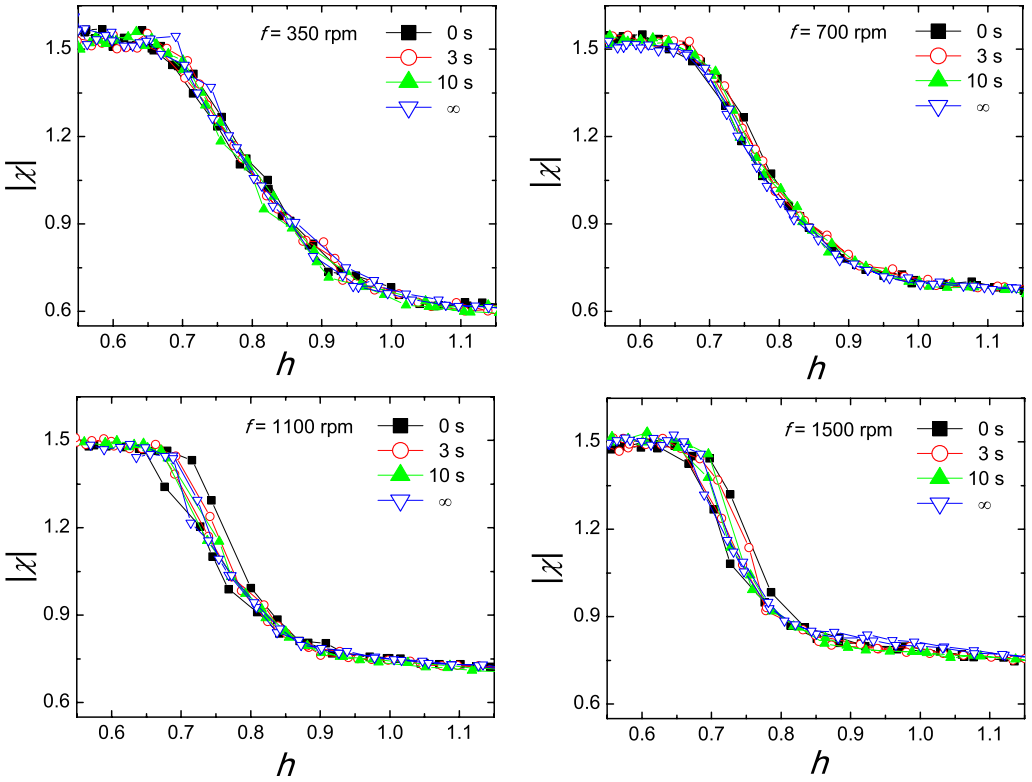

FIG. 4. (Color online) Amplitude of the magnetic susceptibility χ as a function of the reduced magnetic field, $h=H/H_{c0}[1-(T_{sur}/T_c)^2]$, where H_{c0} is the value of the thermodynamic critical field at zero temperature, T_c is the superconducting transition temperature, and T_{sur} is the temperature read by the thermometer at the sample surface when the set temperature is $T_{set}=5$ K and the permanent magnet rotates at different frequencies (from left to right and from top to bottom): $f=350$, 700, 1100, and 1500 rpm. The curves shown in each panel correspond to different values of the time the system waits before each experimental point is measured: $t_w=0$ (solid squares), $t_w=3$ s (open circles), $t_w=10$ s (solid upward triangles), and $t_w\to\infty$ (open downward triangles). Lines are guides to the eye.

out to be smaller than the theoretical value corresponding to this T_{set}, indicating that even in this case the average temperature inside the sample, T_{int}, would be larger than the temperature read by the thermometer at the surface, T_{sur}.

To elucidate the role of the actual sample temperature in the processes just described, the results shown in Fig. 2 are plotted in Fig. 4 by representing $|\chi|$ as a function of a reduced magnetic field defined as $h\equiv H/H_{c0}[1-(T_{sur}/T_c)^2]$, where T_{sur}/T_c is a reduced sample surface temperature calculated for each experimental point. A sharp scaling of the data corresponding to the different values of t_w onto a single curve is observed for the two lowest frequencies, supporting the explanation given above in terms of heating released in the sample by the motion of the normal regions in the IS. A scaling that neat is also observed at the two highest frequencies for $t_w=10$ s (solid upward triangles) and $t_w\to\infty$ (open downward triangles) but it is loosely achieved as the waiting time is reduced down to $t_w=0$ (solid squares). The reason for this time dependence can be understood by considering that the heat released at short waiting times inside the sample along $|\chi|_{asc}(H)$ would not travel to the surface fast enough to establish a stationary state in the whole sample before the magnetic response would be measured along $|\chi|_{des}(H)$. This would mean that the value of T_{sur} read by the thermometer for each point along this branch would never match the actual value of T_{int} and the data would therefore not scale in this representation. The opposite would prevail at $t_w=10$ s, in the sense that the heat released inside the sample along $|\chi|_{asc}(H)$ would have reached the surface by the time the signal would be recorded along $|\chi|_{des}(H)$. In this case, the value of T_{sur} read by the thermometer for each data point would always correspond to the proper thermal equilibrium state of the sample and, as a consequence, the measurements made along $|\chi|_{asc}(H)$ and $|\chi|_{des}(H)$ would superimpose.

To look deeply into the influence of the frequency, the results of Fig. 2 were replotted by grouping the data measured at different values of f for the same value of t_w. Figure 5 shows an example of this representation for $t_w\to\infty$ when $T_{set}=5$ K. Similar results were obtained at finite values of t_w. As in previous figures, the data at low magnetic fields superimpose within the experimental error onto the single master curve that corresponds to the MS. As the magnetic field increases beyond H_c', the data follow four separate curves which intersect somewhere along the way to become upwardly ordered in the NS for increasing values of f. We can try to understand this by considering that Lenz's law, $-d\phi/dt=RI+LdI/dt$, that induces the screening current I when a time varying magnetic flux ϕ threads the sample in the resistanceless, superconducting state, does also apply in the resistive NS. In this case, if the rotating magnetic field is considered as a time oscillating function and its direction and positive orientation are taken as a reference at any time, a complex expression can be derived for the induced magnetic susceptibility in terms of the resistance R and the self-

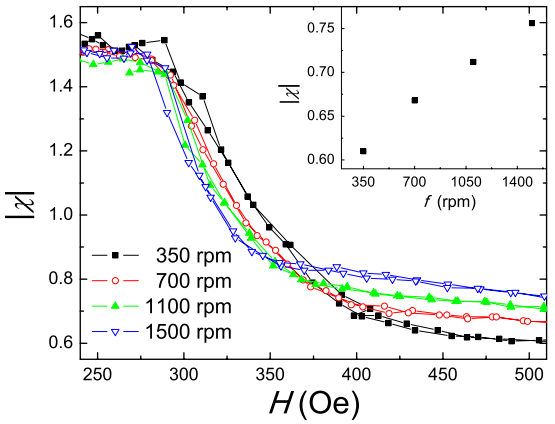

FIG. 5. (Color online) Amplitude of the magnetic susceptibility χ as a function of the magnetic field when the set temperature is $T_{set}=5$ K and the waiting time is $t_w \to \infty$. The four curves correspond to the different values of the frequency of rotation of the permanent magnet: $f=350$ rpm (solid squares), $f=700$ rpm (open circles), $f=1100$ s (solid upward triangles), and $f=1500$ rpm (open downward triangles). The inset shows the frequency dependence of the amplitude of the magnetic susceptibility at $H=500$ Oe. Lines in the main figure are guides to the eye.

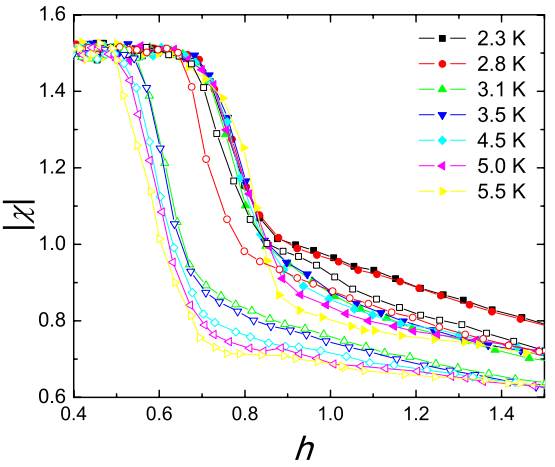

FIG. 6. (Color online) Amplitude of the magnetic susceptibility χ as a function of the reduced magnetic field, $h=H/H_{c0}[1-(T_{sur}/T_c)^2]$, where H_{c0} is the value of the thermodynamic critical field at zero temperature, T_c is the superconducting transition temperature, and T_{sur} is the temperature read by the thermometer at the sample surface for different set temperatures T_{set} between 2.3 and 5.5 K (see legend for details), when the frequency of rotation of the permanent magnet was $f=1500$ rpm. Solid symbols correspond to data measured as the magnetic field increased from zero to its maximum value, while open symbols correspond to data measured all the way back. Lines are guides to the eye.

inductance L of the sample, and the angular frequency of the magnetic field, $\omega=2\pi f$: $\chi_{Lenz}=L\omega/(-L\omega+jR)$.

The low-temperature dependence of R in Pb is ruled by a T^5 law[29,30] that gives an estimate of $10^{-8}-10^{-9}$ Ω, which can be an order of magnitude larger than the values of $L\omega$ than can be calculated at the frequencies of our experiments by approximating the sample either as a single circular loop or as a solenoidal coil. In this case, the resistance becomes dominant and the Lenz contribution to the magnetic susceptibility can be approximated as $\chi_{Lenz} \simeq -jL\omega/R$. This linear frequency dependence is confirmed experimentally in the inset of Fig. 5, where the values of $|\chi|$ for a certain intensity of the magnetic field in the NS ($H=500$ Oe in this case) are plotted as a function of f. This interpretation is further supported by the fact that the phase difference between the two channels when the sample was in the NS stayed always close to $-\pi/2$, indicating the absence of an in-phase term in the magnetic susceptibility that could come from χ_{Lenz}. Finally, a decreasing dependence of H_c as f increases can be also observed in the main figure, just in accordance with the fact that the amount of heat released inside the sample along $|\chi|_{asc}(H)$ also increases with f. In this case, even if $T_{sur}=T_{set}$ for each data point, the deviation of T_{int} from T_{sur} becomes nevertheless increasingly larger and, as a consequence, the actual value of the thermodynamic critical field is reduced with respect to $H_c(T_{sur})$.

Figure 6 presents as a function of the reduced magnetic field the results obtained for the last kind of experiment mentioned above, when the amplitude of the signal was measured for $f=1500$ rpm at several values of T_{set} between 2.3 and 5.5 K, just as the magnetic field changed continuously up and down between zero and its maximum value. Once again, all $|\chi|_{asc}(H)$ curves (solid symbols in the figure) superimpose onto a single initial plateau, corresponding to the MS, and at $h_c' \simeq 0.7$ undergo a progressive decrease along which they split into two distinct sets: the curves for $T_{set} \leq 2.8$ K (set 1, solid circles and squares) stick together while the curves for $T_{set} > 2.8$ K (set 2, all other solid symbols) deviate from set 1 at a certain h value, the higher the T_{set}, the larger such deviation. As the sample gets deeper into the NS, the data of set 2 superimpose again onto a common curve which eventually tends to merge with set 1 at larger intensities of the magnetic field (not shown in the figure). For decreasing values of the magnetic field (open symbols in the figure), the $|\chi|_{des}(H)$ curves regroup in sets 1 and 2, each of which follows a path well below the corresponding $|\chi|_{asc}(H)$ curve and originates a temperature-dependent hysteresis that stretches down to a certain value of the reduced magnetic field ($h \simeq 0.65$ for set 1 and $h \simeq 0.50-0.55$ for set 2), at which the temperature-independent initial plateau corresponding to the MS is regained.

The different behavior observed for the two sets of curves could be an indication that some experimental conditions are changing with temperature. As stated before, the cryostat works under a continuous flow of ^{4}He, so the sample should always be surrounded by gas. However, as the temperature decreases, the inner pressure of the cryostat could allow helium to liquefy and attain a certain level above the sample position. The material would be then immersed in liquid helium, whose thermal conductivity is one order of magnitude larger than that of helium gas,[31] allowing for a prompt absorption of the heat released by the motion of normal zones in the IS. This could be the case for the two curves in set 1, for which the average value of T_{int} would stay always close to T_{set}, as it is actually suggested by the scaling observed in Fig. 6. At any other temperature, the small thermal conductivity of helium gas would hinder the sample from attaining

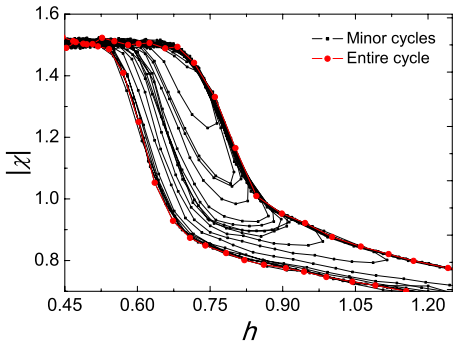

FIG. 7. (Color online) Amplitude of the magnetic susceptibility χ as a function of the reduced magnetic field, $h=H/H_{c0}[1-(T_{sur}/T_c)^2]$, where H_{c0} is the value of the thermodynamic critical field at zero temperature, T_c is the superconducting transition temperature, and T_{sur} is the temperature read by the thermometer at the sample surface when the set temperature was $T_{set}=3.5$ K and the frequency of rotation of the permanent magnet was $f=1500$ rpm. The large solid circles correspond to the full hysteresis cycle measured as the magnetic field varies up and down between zero and its maximum value, and the different small solid squares correspond to minor loops measured by stopping at different points along the ascending branch of the entire cycle and reducing the intensity of the magnetic field back to zero. Lines are guides to the eye.

a thermal equilibrium before each data point is measured in which case, T_{int} would deviate from T_{set} and the scaling would be far from being achieved, as it is the case for the curves in set 2.

The fact that both sets tend to a common constant value at large magnetic fields can be explained just by considering that a large amount of heat should be expected to be released inside the sample at these intensities and so the value of T_{int} and, therefore, the resistance in the denominator of the approximate expression of χ_{Lenz} would become large enough to make this contribution vanish and leave only the residual signal due to the lack of a precise compensation between the two detection coils. As for the large hysteresis observed at each T_{set} in set 2, the reason could be the continuous data-acquisition process, for in these experimental conditions the heat released inside the sample along $|\chi|_{asc}(H)$ would not have time enough to reach the surface at the moment each experimental point is measured along $|\chi|_{des}(H)$, in a way similar to that described before for the experiments performed at $t_w=0$.

To explore further the dynamics of the IS in this kind of experiment, the sample was submitted at each T_{set} to a large collection of subsequent minor runs for both ascending and descending values of the magnetic field. Figure 7 shows an example of one of those collections (small solid squares) measured at $T_{set}=3.5$ K for $f=1500$ rpm, together with the corresponding entire cycle that already appeared in Fig. 6 (large solid circles). Each minor loop was measured running the magnetic field up along $|\chi|_{asc}(H)$, suddenly stopping at a certain value, H_{turn}, and decreasing afterward the magnetic field down to zero. Similar results were obtained by stopping at different H_{turn} values along $|\chi|_{des}(H)$ and increasing afterward the magnetic field up to the maximum value. It is remarkable the fact that, no matter how small H_{turn} might be, a hysteresis sets up always, the larger the value of this magnetic field, the wider the corresponding cycle. This is in agreement with the fact that the time it takes to measure $|\chi|_{asc}(H)$ increases with H_{turn} and so does in accordance the time the heat is released in the sample during the motion of the normal zones in the IS. As a consequence, T_{int} deviates increasingly from T_{sur} as H diminishes and the separation of the decreasing branch of the loop from $|\chi|_{asc}(H)$ grows accordingly. It is worth noticing there is a limit on the width of the minor loops set by $|\chi|_{des}(H)$ in the sense that the highest dissipation would occur when the magnetic field is cycled up to and down from its maximum value in which case the total time it takes to perform the complete measurement would be the largest.

To summarize, the properties of the IS and the NS of a pure type-I superconducting lead sphere have been investigated under magnetic fields of up to 1 T rotating at frequencies of up to 1500 rpm. Different experimental procedures have been followed that differ in the time elapsed between the application of a certain magnetic field intensity and the measurement of the corresponding magnetic response of the sample. This waiting time, together with the frequency of rotation of the magnet and the variation in the temperature of the sample while sweeping the magnetic field up and down between zero and its maximum value, has proven relevant for the reduction in the thermodynamic critical field and the occurrence of hysteresis in the magnetic field dependence of the amplitude of the magnetic susceptibility. These effects have been ascribed to the deviation of the temperature of the sample with respect to the temperature of the bath as a consequence of the heat released during the motion of normal zones in the intermediate state of the sample subject to the rotation of the magnetic field. In addition, the magnetic signal in the normal state presents an increasing linear dependence on frequency that has been attributed to the dominance of the resistive term upon the inductive term in the expression of Lenz's law under a magnetic field that oscillates with time.

In a recent work[32] the authors studied topological magnetic irreversibilities in superconducting lead samples of various shapes under static magnetic fields and corroborated the previous result[9] that a tubular structure should be the equilibrium ground state for the flux configuration in pinning-free spheres while the presence of geometrical barriers is responsible for the occurrence of magnetic hysteresis in disks and cylinders. An exhaustive exploration of samples of these two shapes is currently underway in order to elucidate the role that the anisotropy of the sample might play in the dynamics of the normal zones in the IS under rotating magnetic fields. Further experiments based on the implementation of a magneto-optical setup or the use of micro-Hall sensor arrays inside the cryostat should be pursued to determine the actual flux configuration in samples of all shapes.

S.V. acknowledges support from Ministerio de Ciencia e Innovación. J.M.H. acknowledges support from Ministerio de Educación y Ciencia and Universitat de Barcelona. A. G.-S. acknowledges support from Universitat de Barcelona. This work was financially supported by the Spanish Government Projects No. MAT2005-06162 and No. MAT2008-04535.

*agarciasan@ub.edu

[1] R. E. Goldstein, D. P. Jackson, and A. T. Dorsey, Phys. Rev. Lett. **76**, 3818 (1996).
[2] H. Bokil and O. Narayan, Phys. Rev. B **56**, 11195 (1997).
[3] A. T. Dorsey and R. E. Goldstein, Phys. Rev. B **57**, 3058 (1998).
[4] A. Cebers, C. Gourdon, V. Jeudy, and T. Okada, Phys. Rev. B **72**, 014513 (2005).
[5] C. Gourdon, V. Jeudy, and A. Cebers, Phys. Rev. Lett. **96**, 087002 (2006).
[6] L. D. Landau, Zh. Eksp. Teor. Fiz. **7**, 371 (1937); L. Landau, Nature (London) **141**, 688 (1938).
[7] R. Prozorov, R. W. Giannetta, A. A. Polyanskii, and G. K. Perkins, Phys. Rev. B **72**, 212508 (2005).
[8] M. Menghini and R. J. Wijngaarden, Phys. Rev. B **75**, 014529 (2007).
[9] R. Prozorov, Phys. Rev. Lett. **98**, 257001 (2007).
[10] R. Prozorov, A. F. Fidler, J. R. Holberg, and P. C. Canfield, Nat. Phys. **4**, 327 (2008).
[11] J. R. Hoberg and R. Prozorov, Phys. Rev. B **78**, 104511 (2008).
[12] R. Prozorov and J. R. Hoberg, J. Phys.: Conf. Ser. **150**, 052217 (2009).
[13] W. F. Love, R. F. Blunt, and P. B. Alers, Phys. Rev. **76**, 305 (1949).
[14] A. Wexler and W. S. Corak, Phys. Rev. **78**, 260 (1950).
[15] P. B. Alers, J. W. McWhirter, and C. F. Squire, Phys. Rev. **84**, 104 (1951).
[16] A. F. Hildebrandt, Phys. Rev. Lett. **12**, 190 (1964).
[17] M. Menghini and R. J. Wijngaarden, Phys. Rev. B **72**, 172503 (2005).
[18] *Alfa Aesar* 42691 (lead rod, 6.35 mm diameter).
[19] *Magnetic Properties Measurement System, Quantum Design*, San Diego, CA.
[20] M. Tinkham, *Introduction to Superconductivity*, 2nd ed. (Dover, New York, 2004), p. 3.
[21] The equipment was designed by our group (Patent Application No. ES2261050) and was developed by *Oxford Instruments*, Abingdon, UK.
[22] A. Hernández-Mínguez, C. Carbonell-Cortés, R. Amigó, J. M. Hernandez, J. Tejada, and E. M. Chudnovsky, Appl. Phys. Lett. **91**, 202502 (2007).
[23] G10 glass reinforced epoxy.
[24] *Lake Shore Cryogenics, Inc.*, Westerville, OH.
[25] *Agilent Technologies*, Santa Clara, CA; 54621A model.
[26] The difference of two sine with similar phases is proportional to a cosine with this same phase, hence the $\sim \pm \pi/2$ phase difference between the two channels.
[27] *Keithley Instruments, Inc.*, Cleveland, OH; 2400 model.
[28] J. A. Osborn, Phys. Rev. **67**, 351 (1945).
[29] G. J. Van Den Berg, Physica (Amsterdam) **14**, 111 (1948).
[30] A. Eiling and J. S. Schilling, J. Phys. F: Met. Phys. **11**, 623 (1981).
[31] F. Pobell, *Matter and Methods at Low Temperatures*, 3rd ed. (Springer-Verlag, Berlin, 2007), p. 23.
[32] S. Vélez, C. Panadès-Guinart, G. Abril, A. García-Santiago, J. M. Hernandez, and J. Tejada, Phys. Rev. B **78**, 134501 (2008).